Contents lists available at ScienceDirect

Digestive and Liver Disease

Oncology

Diffusion-weighted magnetic resonance imaging predicts malignant potential in small hepatocellular carcinoma

Shusuke Okamura [a,*], Shuji Sumie [a], Tatsuyuki Tonan [b], Masahito Nakano [a],
Manabu Satani [a], Shigeo Shimose [a], Tomotake Shirono [a], Hideki Iwamoto [a], Hajime Aino [a],
Takashi Niizeki [a], Nobuyoshi Tajiri [a], Ryoko Kuromatsu [a], Koji Okuda [c],
Osamu Nakashima [d], Takuji Torimura [a]

[a] Division of Gastroenterology, Department of Medicine, Kurume University School of Medicine, Kurume, Fukuoka, Japan
[b] Department of Radiology, Kurume University School of Medicine, Kurume, Fukuoka, Japan
[c] Division of Hepato-Biliary-Pancreatic Surgery, Kurume University School of Medicine, Kurume, Fukuoka, Japan
[d] Department of Clinical Laboratory Medicine, Kurume University School of Medicine, Kurume, Fukuoka, Japan

ARTICLE INFO

ABSTRACT

Background: Poor differentiation and microvascular invasion are indicators of poor outcome after hepatectomy for patients with small hepatocellular carcinoma (HCC).
Aims: We investigated whether gadoxetic acid-enhanced and diffusion-weighted magnetic resonance imaging (MRI) could predict these factors before hepatectomy.
Methods: Between July 2008 and April 2012, 75 patients who underwent hepatectomy for small HCCs (diameter: ≤3 cm, tumor number: ≤3) were consecutively enrolled. In gadoxetic acid-enhanced MRI, the signal intensity in the tumor was corrected to that in the paraspinous muscles, and the relative enhancement was calculated. In diffusion-weighted imaging, we measured the apparent diffusion coefficient (ADC). We then investigated the correlations between relative enhancement or ADC and histological grade, microvascular invasion and recurrence-free survival.
Results: Poorly differentiated HCCs showed significantly lower ADC than well-differentiated and moderately differentiated HCCs. There was no significant difference in the hepatobiliary phase. Only ADC was an independent predictor of microvascular invasion, and the best cut-off point of its prediction was 1.175×10^{-3} mm^2/s. Additionally, the recurrence-free survival was significantly shorter in low-ADC group than in high-ADC group.
Conclusion: ADC is useful for predicting poorly differentiated HCCs and microvascular invasion, and low ADC is associated with increased recurrence risk for small HCCs after hepatectomy.

© 2016 Editrice Gastroenterologica Italiana S.r.l. Published by Elsevier Ltd. All rights reserved.

1. Introduction

Hepatocellular carcinoma (HCC) is one of the most common malignancies in the world [1]. Recent advances in imaging procedures and surveillance programs for high-risk patients have led to increased detection of early-stage HCC, resulting in an increase in identification of patients in whom curative therapy is possible. However, the long-term survival of HCC patients remains unsatisfactory, owing to the high frequency of intra- and extra-hepatic recurrence.

Poor differentiation and microvascular invasion (MVI) indicate malignant potential and are recognized as risk factors for early recurrence of HCC [2,3]. Previously, we reported that MVI results in frequent intrahepatic metastasis and is the most important predictor of recurrence [2]. Therefore, identification of MVI could help in the selection of appropriate surgical resection, improving cure rates. However, identification of MVI requires histological examination, which limits its usefulness for pretreatment assessment. Additionally, aspiration biopsy is an invasive procedure that has some drawbacks, such as sampling error and needle-track seeding of HCC [4,5]. Therefore, development of a non-invasive procedure for pretreatment assessment of malignant potential in HCC is crucial.

* Corresponding author at: Division of Gastroenterology, Department of Medicine, Kurume University School of Medicine, 67 Asahimachi, Kurume-shi, Fukuoka 830-0011, Japan. Tel.: +81 942 31 7561; fax: +81 942 34 2623.
E-mail address: okamura_shyuusuke@kurume-u.ac.jp (S. Okamura).

Gadoxetic acid is a liver-specific contrast agent used in magnetic resonance imaging (MRI), which has improved the detectability of HCC, including early-stage HCC, which is not easily detected using only conventional blood flow evaluation [6]. Moreover, gadoxetic acid-enhanced MRI has also been reported to be useful in the prediction of malignant potential. Some authors have reported the correlation between the histological grade and the signal intensity (SI) of the tumor in the hepatobiliary phase [7–9]. Moreover, there is a correlation between the macroscopic type of HCCs and MVI [2,10–12], and the hepatobiliary phase has been shown to be useful for gross morphological evaluation [11].

Diffusion-weighted imaging (DWI), an MRI technique, is based on the restriction of water molecule movement. Apparent diffusion coefficient (ADC) measurements with DWI obtained at two or more b-values allows quantitative analysis of diffusion [13]. In tumorous tissues, it is thought to detect the restriction of the motion of water molecules that is associated with the decrease in the extracellular space caused by high cellularity [14]. DWI may be able to provide additional information for the detection of tumors or the differentiation of HCC from dysplastic nodules [15,16]. Recently, several studies have reported that DWI examination could predict both histological grade and MVI [17–24]. However, for small HCCs, the correlation between MRI SIs and malignant potential or postoperative recurrence is unclear.

Here, we investigated whether quantitative gadoxetic acid-enhanced and DWI MRI could predict the histological grade and MVI of small HCCs before hepatic resection, and examined which modality was the most useful in this respect. Additionally, we identified the relationship between preoperative quantitative MRI and the recurrence risk of small HCCs.

2. Materials and methods

2.1. Patients

In this retrospective study, we consecutively enrolled 75 initial HCC patients (tumor diameter: ≤3 cm, tumor number: ≤3) without extrahepatic metastasis or macrovascular invasion, who had undergone surgical resection at Kurume University Hospital from July 2008 to April 2012. All patients underwent gadoxetic acid-enhanced and DWI MRI before hepatic resection. Informed consent was obtained from each patient, and the protocol conformed to the Declaration of Helsinki and was approved by our institutional review board.

The study included 54 males and 21 females, with a median age of 67 years (range: 32–83 years). Nineteen patients were positive for hepatitis B virus infection and 50 patients were positive for hepatitis C virus infection. Liver cirrhosis was present in 37 patients. Fifty-nine patients had one HCC lesion, 12 patients had two HCC lesions, and four patients had three HCC lesions. The median tumor diameter was 21 mm (range: 7–30 mm). The median level of alpha-fetoprotein (AFP) was 13.3 ng/ml (range: 1.4–6278 ng/ml), and the median level of des-gamma-carboxy prothrombin (DCP) was 34 mAU/ml (range: 11–1939 mAU/ml; excluding two patients on warfarin).

2.2. MRI protocol

Fifty-four patients were examined with 1.5 T MRI system (MAGNETOM Symphony Advanced; SIEMENS, Erlangen, Germany) and 21 patients were examined with 3.0 T MRI system (Signa HDx, GE Healthcare, Milwaukee, WI, USA). The median time from MRI examination to surgery was 27 days (range: 1–85 days).

With 1.5 T MRI, pre-contrast and post-contrast images were obtained using T1-weighted volumetric interpolated breath-hold examination (VIBE) sequence with fat suppression (repetition time [TR], 3.6 ms; echo time [TE], 1.73 ms; slice thickness, 5 mm; flip angle [FA], 15°; field of view [FOV], 36 cm; matrix size, 202 × 256; acceleration factor, 2; gap, 0 mm). With 3.0 T MRI, images were obtained using T1-weighted liver acceleration volume acquisition (LAVA) sequence with fat suppression (TR, 3.3 ms; TE, 1.6 ms; slice thickness, 2 mm; FA, 12°; FOV, 36 cm; matrix size, 320 × 190; asset factor, 2; gap, 0 mm).

For the dynamic study, 0.025 mmol/kg body weight of gadoxetic acid disodium (Primovist, Bayer Schering Pharma, Berlin, Germany) was administered as an intravenous bolus at a rate of 2 ml/s, followed by flushing with 20 ml of saline solution, using a mechanical injector. The arterial phase, portal venous phase, equilibrium phase, and hepatobiliary phase were obtained at 30 s, 90 s, 4 min, and 20 min, respectively, on 1.5 T MRI, and at 15 s, 80 s, 4 min, and 20 min on 3.0 T MRI, after administration of gadoxetic acid disodium.

DWI was performed in the transverse plane by a respiratory-triggered combination of single-shot spin-echo echo-planar imaging with a chemical shift-selective pulse. The imaging parameters for DWI on 1.5 T MRI were as follows: repetition time, 2000 ms; echo time, 81 ms; directions of the motion-probing gradient, three orthogonal axes; gradient factor b-values of 0 and 1000 s/mm^2; 350-mm FOV; 128 × 88 rectangular matrixes; 9-mm-thick sections; 1-mm intersection gap; four signals acquired. The imaging parameters for DWI on 3.0 T MRI were as follows: repetition time, 5000 ms; echo time, 68 ms; gradient factor b-values of 0 and 1000 s/mm^2; 380-mm FOV; 128 × 88 rectangular matrixes; 7-mm-thick sections; 1-mm intersection gap; four signals acquired. ADC maps were obtained automatically by two images of b-values 0 and 1000 s/mm^2.

2.3. Image analysis

In all cases, tumors could be confirmed in the hepatobiliary phase; therefore, tumor diameter was measured in this phase. If patients had two or three HCC nodules, we evaluated the largest one; therefore, only one nodule was examined per patient. In gadoxetic acid-enhanced MRI, the SI of the tumor was measured using a region of interest (ROI) on pre-contrast and post-contrast images for the quantitative analysis. To avoid partial volume calculation errors, the ROI of each tumor was placed at the slice where the tumor was best visualized (almost equal to largest diameter of the tumor), with a maximum round or oval area within the tumor. To exclude the influence of the environment at the time of the examination and the composition of the patient, the SI of the tumors was corrected by the SI of the paraspinous muscles (liver-to-muscle signal intensity [LMSI]), which was also measured in the ROI (about 100 mm^2), in the same slice. The relative enhancement (RE) was calculated as follows: RE = (Post LMSI − Pre LMSI)/Pre LMSI [25]. Furthermore, RE on the arterial phase was marked as AP-RE and RE on the hepatobiliary phase was marked as HBP-RE. The ADC was measured with the ROI on the ADC map, with reference to the DWI, as with gadoxetic acid-enhanced MRI (Fig. 1). When the tumor was not visible on DWI, ADC measurement was performed by using the triangulation function of Picture Archiving and Communication System (PACS). This function identifies the same point on different images relative to a specific point on image; the identified point corresponds to the same area of the tumor in the hepatobiliary phase. The ROI in the liver parenchyma was placed in the right hepatic lobe with the size of 200–500 mm^2, excluding major vessels and artifacts.

MRIs were evaluated separately on the workstation (GE Healthcare Centricity) by a hepatologist with 11 years of experience (S.O.) and an abdominal radiologist with 19 years of experience (T.T.), blinded to the patients' clinical records, and the mean value of their
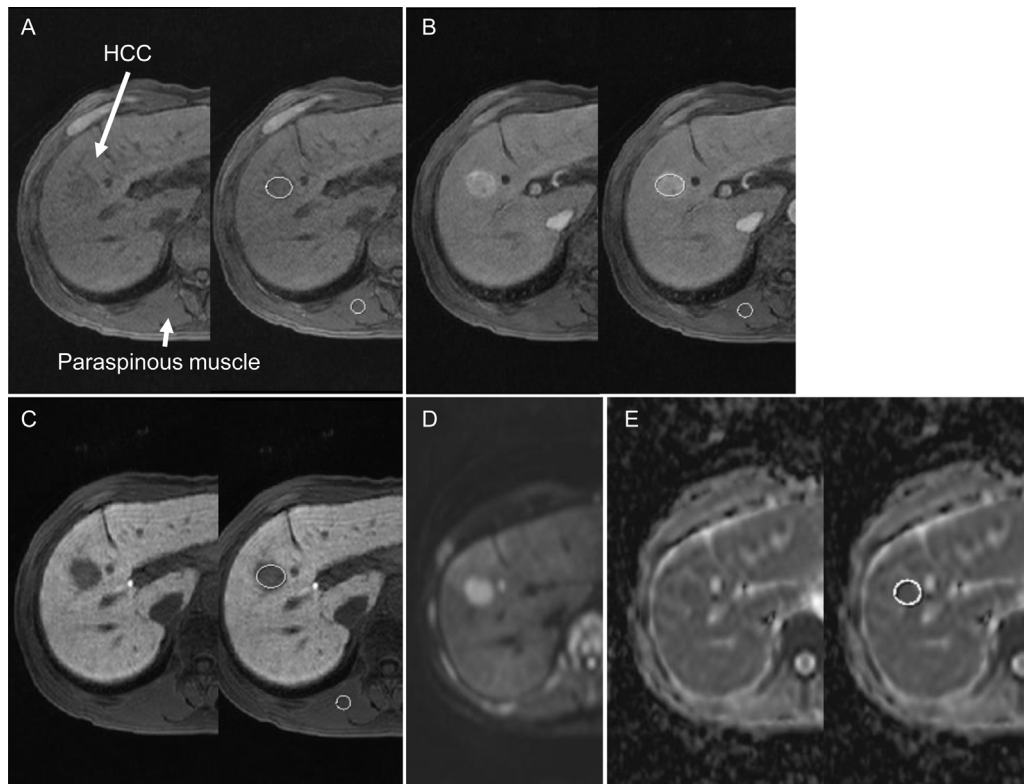
Fig. 1. A pre-contrast image (A), arterial phase image (B), hepatobiliary phase image (C), diffusion-weighted image (DWI; *b*-values of 1000 s/mm^2) (D), and ADC map image (E) of the same patient are shown. The signal intensities of the tumor and paraspinous muscles were measured using a region of interest (ROI) on the pre-contrast and post-contrast images. The ADC was also measured using the ROI on the ADC map, with reference to the DWI.

measurements was used in analysis. ADC assessment within the liver may be difficult, and variations in ADC values may be related to motion artifacts and to the HCC position within the liver. Hence, we calculated the interobserver variation to confirm the reproducibility of the evaluations.

2.4. Histopathological evaluation

The resected liver tissues were cut into serial 2- to 3-mm-thick specimens and fixed in 10% formalin to facilitate careful gross and histopathological examinations. Each specimen was embedded in paraffin, cut into 4-μm-thick sections, and stained with hematoxylin and eosin. Histological grade was based on the criteria of the World Health Organization [26]. When the evaluated nodule comprised two areas of different histological grades, the worse histological grade was recorded. MVI was defined as a microscopic tumor invasion identified in the portal vein and the hepatic vein of the surrounding liver tissue that was contiguous with the tumor edge. Non-cancerous liver tissue was inspected for evidence of cirrhosis.

2.5. Statistical analysis

Continuous variables were expressed as median (range). Chi-square test or Fisher's exact test was used to analyze the correlation between categorical variables and MVI. Wilcoxon's test was used to analyze the correlation between continuous variables and MVI, as well as the correlation between the degree of histological grade and AP-RE value, HBP-RE value, and ADC. Logistic regression analysis was used to assess the study parameters for the prediction of MVI and to calculate the odds ratio (OR) and 95% confidence interval (95% CI). Variables with significant *P*-values in univariate analysis were used for multiple logistic regression analysis. The best

cut-off points of MRI SIs were calculated from receiver operating characteristic (ROC) curves to identify the presence of MVI. The recurrence-free survival (RFS) rate was calculated from the date of surgery to the appearance of local or distant tumor progression. The RFS rate was evaluated using the Kaplan–Meier method, and the log-rank test was used to compare the patient groups. Bland–Altman plots and the Pearson correlation coefficient were used to assess the interobserver agreement of the ADC measurements on the ADC map. *P*-values less than 0.05 were considered to be statistically significant. JMP version 11 (SAS Institute, Inc., Cary, NC, USA) software was used for all analyses.

3. Results

3.1. Correlations between the histological grade and AP-RE, HBP-RE, and ADC in HCC

Eight of the 75 HCC nodules examined were well-differentiated (WD) HCCs, 52 were moderately differentiated (MD) HCCs, and 15 were poorly differentiated (PD) HCCs. Sixty-three HCCs had a typical contrast pattern (WD/MD/PD: 6/47/10), and 12 had a nontypical contrast pattern (WD/MD/PD: 2/5/5). Fig. 2 shows the relationships between the AP-RE value, HBP-RE value, and ADC and each histological grade. The median AP-RE value was 0.288 (range: 0.019–0.732), 0.751 (range: 0.164–2.016), and 0.74 (range: 0.036–1.398) in WD HCCs, MD HCCs, and PD HCCs, respectively. The value for WD HCCs was significantly lower than the values for MD and PD HCCs, which did not differ significantly.

The median HBP-RE value was 0.287 (range: 0.019–0.478), 0.168 (range: 0.003–1.403), and 0.191 (range: 0.006–0.509) in WD HCCs, MD HCCs, and PD HCCs, respectively. These differences were not significant.
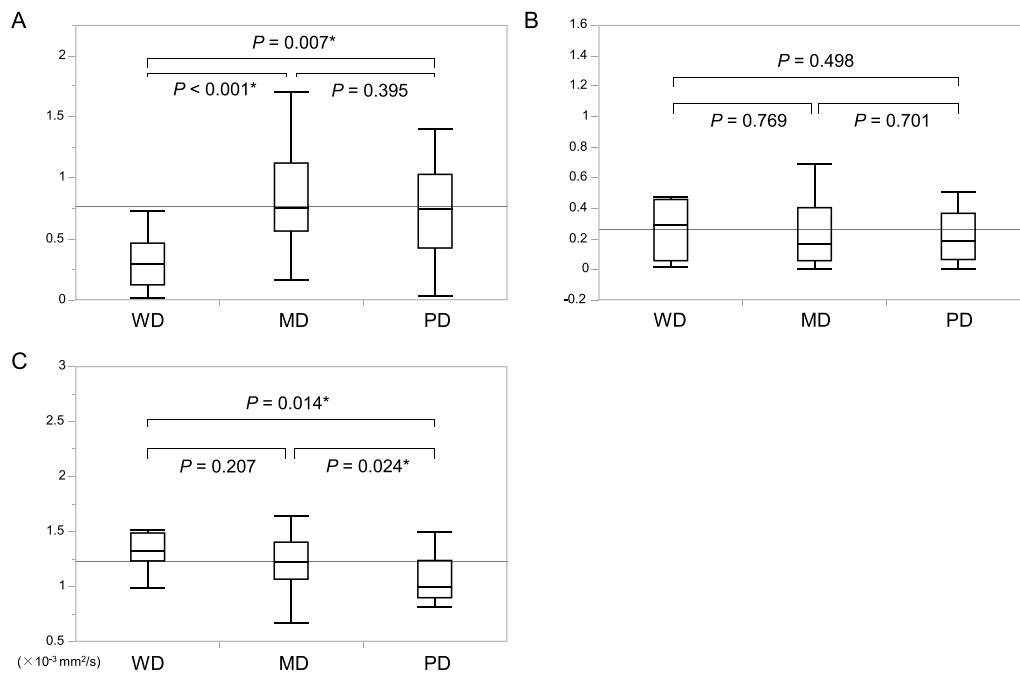
Fig. 2. Correlations between the histological grade and AP-RE (A), HBP-RE (B), and ADC (C) in HCCs. The median AP-RE values were 0.288, 0.751, and 0.74, the median HBP-RE values were 0.287, 0.168, and 0.191, and the ADC values were 1.328×10^{-3} mm^2/s, 1.218×10^{-3} mm^2/s, and 0.995×10^{-3} mm^2/s in WD HCCs, MD HCCs, and PD HCCs, respectively.

In DWI, we evaluated 73 HCCs (two MD HCCs with a typical contrast pattern were excluded from the analysis because it was difficult to determine their ADCs from their MRI owing to strong artifacts). The median ADC values of nodules with typical and nontypical contrast patterns were 1.21 (range: $0.67–2.25) \times 10^{-3}$ mm^2/s and 1.24 (range: $0.82–2.97) \times 10^{-3}$ mm^2/s, respectively; this difference was not significant ($P = 0.947$). The median ADC value was 1.328 (range: $0.985–2.25) \times 10^{-3}$ mm^2/s, 1.218 (range: $0.665–2.97) \times 10^{-3}$ mm^2/s, and 0.995 (range: $0.815–1.485) \times 10^{-3}$ mm^2/s in WD HCCs, MD HCCs, and PD HCCs, respectively. PD HCCs had significantly lower ADCs than did WD and MD HCCs, whose ADCs did not differ significantly.

3.2. Correlations between MVI and AP-RE, HBP-RE, and ADC in HCCs

Thirty-three of the 75 HCC nodules presented with MVI. Table 1 shows the correlations between several clinical or radiological characters and MVI by univariate analysis. Levels of AFP and DCP were significantly higher and PD HCCs were more dominant in patients with MVI than in those without.

For SI evaluation of preoperative MRI, only the ADC correlated with MVI. We also calculated the ROC curves of the AP-RE value, HBP-RE value, and ADC for the prediction of MVI. The best cut-off point of each ROC curve was used to divide the patients in the Kaplan–Meier analysis (Fig. 3). The AUC in the AP-RE, HBP-RE, ADC ROC curves were 0.629, 0.548, and 0.772, respectively. For predicting MVI, the best cut-off points for AP-RE value, HBP-RE value, and ADC were 0.946, 0.451, and 1.175×10^{-3} mm^2/s, respectively. The sensitivity, specificity, and diagnostic accuracy of ADC for the prediction of MVI were 75.8%, 77.5%, and 76.6%, respectively. Multiple logistic regression analysis showed that ADC was the only significant independent predictor of the presence of MVI ($P < 0.001$, OR: 8.37, 95% CI: 2.67–29.65, Table 2). Based on this result, we determined the ADCs in a small subgroup of nodules up to 2 cm ($n = 34$, WD/MD/PD: 4/22/8). Interestingly, MVI were observed in 14 cases (41%). Even in this small subgroup, the median ADC was significantly lower in nodules with MVI (1.07 [range: $0.76–1.49] \times 10^{-3}$ mm^2/s) than in those without MVI (1.30

Table 1
Patient characteristics according to the presence or absence of microvascular invasion.

Characteristic	MVI (−)	MVI (+)	*P*-value
Age (years)	69 (33–83)	64 (32–83)	0.223
Gender (male/female)	28/14	26/7	0.305
Background liver (non-cirrhotic/cirrhotic)	20/22	18/15	0.552
Number of tumors (single/2–3)	36/6	23/10	0.154
Tumor size (mm)	20.5 (7–30)	21 (11–30)	0.822
AFP (ng/ml) ($\leq$20/>20)	29/13	13/20	0.01
DCP (mAU/ml) ($\leq$100/>100)	33/8	17/15	0.013
Histological grade (well + moderately differentiated/poorly differentiated)	39/3	21/12	0.003
AP-RE	0.674 (0.019–2.016)	0.849 (0.036–1.556)	0.057
HBP-RE	0.182 (0.003–1.403)	0.189 (0.006–0.567)	0.478
ADC value ($\times 10^{-3}$ mm^2/s)	1.31 (0.665–2.97)	1.08 (0.74–1.57)	<0.001

Continuous variables are expressed as median (range).

MVI: microvascular invasion; AFP: alpha-fetoprotein; DCP: des-gamma-carboxy prothrombin; AP-RE: relative enhancement on arterial phase; HBP-RE: relative enhancement on hepatobiliary phase; ADC: apparent diffusion coefficient.
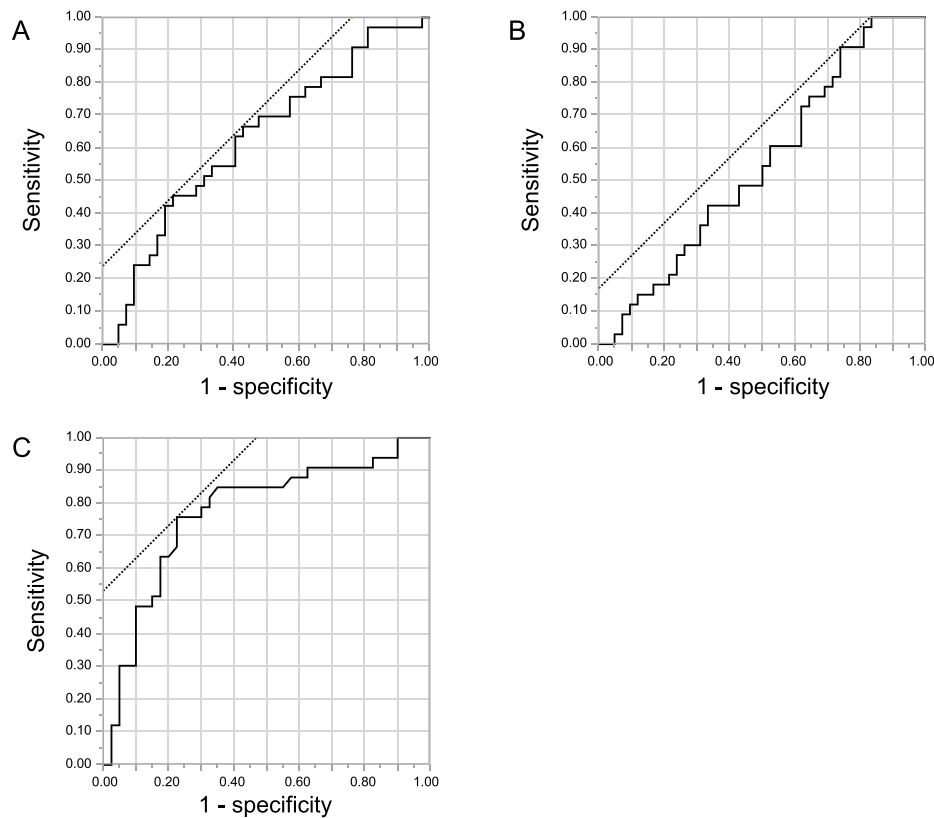
Fig. 3. Receiver operating characteristic (ROC) curve of AP-RE value (A), HBP-RE value (B) and ADC value (C) for the prediction of MVI. The AUC values were (A) 0.629, (B) 0.548, and (C) 0.772, respectively.

[range: 0.67–2.25] $\times 10^{-3}$ mm^2/s] ($P = 0.041$). The best cut-off value for predicting MVI was 1.15×10^{-3} mm^2/s with an AUC of 0.711. The sensitivity and specificity for the prediction of MVI were 78.6% and 65.0%, respectively.

3.3. Correlations between RFS and AP-RE, HBP-RE, and ADC

The AP-RE value, HBP-RE value, and ADC were divided into two groups according to the best-cut off point on the ROC curve (AP-RE: high AP-RE value group [>0.946] and low AP-RE value group [≤0.946]; HBP-RE: high HBP-RE value group [>0.451] and low HBP-RE value group [≤0.451]; ADC: high ADC group [>1.175 × 10^{-3} mm^2/s] and low ADC group [≤1.175 × 10^{-3} mm^2/s]). Kaplan–Meier curves for the RFS rate in each group are shown in Fig. 4. The RFS rate was significantly lower in the low ADC group than in the high ADC group ($P = 0.039$). There were no significant correlations between RFS and AP-RE values or the HBP-RE value.

Table 2
Independent predictors of microvascular invasion by multiple logistic regression analysis.

	OR (95% CI)	P-value
AFP (ng/ml) (≤20/>20)	2.55 (0.71–9.75)	0.153
DCP (mAU/ml) (≤100/>100)	3.11 (0.89–11.76)	0.076
Histological grade (well to moderately differentiated/poorly differentiated)	3.06 (0.59–19.22)	0.185
ADC (×10^{-3} mm^2/s) (≤1.175/>1.175)	8.37 (2.67–29.65)	<0.001

OR: odds ratio; CI: confidence interval; AFP: alpha-fetoprotein; DCP: des-gamma-carboxy prothrombin; ADC: apparent diffusion coefficient.

3.4. Interobserber agreement for ADC assessment

In the Bland–Altman analysis, the mean differences (standard deviations) in the ADCs were 0.07 (7%) and 0.09 (6%) in the nodules and liver parenchyma, respectively. There was no correlation between the average and the difference in the ADC measurements by the two independent observers (Pearson coefficient: $r = 0.18$, $P = 0.133$ and $r = 0.04$, $P = 0.744$ in the nodules and liver parenchyma, respectively). Bland–Altman plots showed no proportional or fixed bias in the ADC measurement, and the correlation between the ADC measurements by the observers was significant (Pearson coefficient: $r = 0.96$, $P < 0.001$ and $r = 0.74$, $P < 0.001$ in the nodules and liver parenchyma, respectively).

4. Discussion

In terms of the relationship between the histological grade and SI of MRI, MD and PD HCCs had significantly higher AP-RE values than did WD HCCs, but MD HCCs and PD HCCs did not differ significantly. HCC is believed to result from multistep carcinogenesis. Early HCC is substantially well differentiated and shows a hypovascular pattern in the arterial phase of imaging studies, due to a decreased arterial blood flow. As the tumor grows, the hypovascular early HCC changes into a hypervascular lesion, due to an increase in abnormal arterial flow [27]. Thus, MD and PD HCCs usually show hypervascularity. Therefore, the AP-RE values in our study reflect intratumoral arterial blood flow and hence are useful only for differentiating WD HCCs from MD or PD HCCs.

In human HCC, gadoxetic acid is mainly taken up through the hepatocyte membrane organic anion-transporting polypeptide 8 (OATP8) [28,29], and a decreased expression of OATP8 shows up as hypointensity as compared with the liver background in the
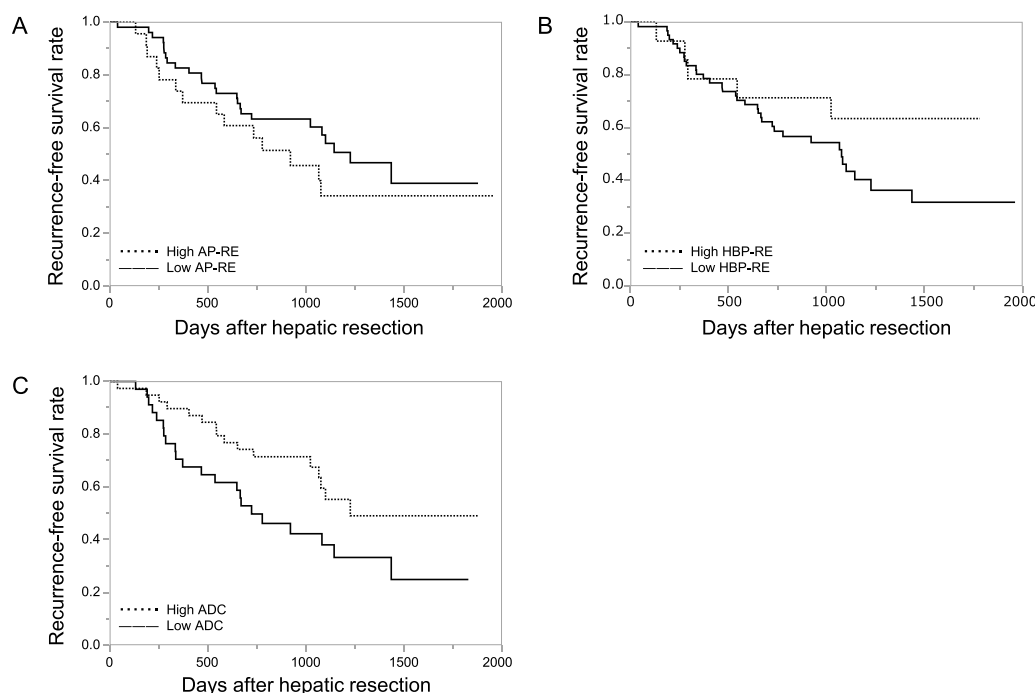
Fig. 4. Comparison of clinical recurrence-free survival (RFS) rate for particular AP-RE values (A), HBP-RE values (B), and ADCs (C). The RFS rate of the low ADC group was significantly lower than that of the high ADC group (*P* = 0.039). There were no significant differences in the RFS of the high and low AP-RE value group and HBP-RE value group (*P* = 0.28 and *P* = 0.173, respectively).

hepatobiliary phase of gadoxetic acid-enhanced MRI [29]. The SI of the tumor in hepatobiliary phase appears to decrease with the progression of the histological grade of HCC [7–9], and Kitao et al. have reported that the expression of OATP8 in HCC decreases significantly during multistep carcinogenesis, except in atypical HCCs that show hyperintensity as compared with the liver background [7].

In the current study, there were no significant differences between the HBP-RE value in tumors of different histological grades. This finding may differ from those of previous reports because, in the current study, we included eight nodules (all MD HCCs) exhibiting iso-SI or high SI compared with the liver background in qualitative evaluation in the hepatobiliary phase. Moreover, there was an overlap of different histological grades in some tumors, including nontypical areas that re-acquired OATP8 expression during multistep carcinogenesis [30]. Another reason for the discrepancies may be our focus on tumors ≤3 cm, or the use of a different evaluation method.

Furthermore, we found that PD HCCs had significantly lower ADCs than did WD and MD HCCs. Several previous studies have evaluated ADCs by using an ROI for predicting the histological grade of HCC [17–21]. Nasu et al. reported no correlation between histological grade and ADC when they placed the ROI in the slice going through the center of each tumor [20]. On the other hand, Nishie et al. placed the ROI on the solid region where ADC was considered to be the lowest in the entire tumor, while Nakanishi et al., who employed the ROI with the minimum ADC, reported that PD HCCs had significantly lower ADCs than did WD and MD HCCs [17,18]. Thus, we obtained the same results as Nishie et al. and Nakanishi et al., although the evaluation method we used was most similar to that of Nasu et al. The histological grade of HCCs depends on the tumor cellularity and structural atypia [31]. Tumor cellularity, nuclear/cytoplasmic ratio, and intracytoplastic organelles increase as the histological grade progresses, and may more markedly restrict diffusion [21,31]. Nasu et al. evaluated tumors that included relatively large nodules (median: 2.9 cm,

range: 0.8–15 cm), which may have included necrotic and hemorrhagic areas with a high ADC. In our study, we evaluated small tumors (<3 cm), in which necrosis and hemorrhage was rare, and therefore would have had a minimal effect on ADC measurement.

In previous reports, tumor size, DCP level, and histological grade were suggested to be useful preoperative predictors for MVI [10,32,33]. Our multiple logistic regression analysis showed only the ADC was an independent predictor.

Several reports have suggested that tumors with non-smooth margins, such as single nodular tumors with an extranodular growth type and confluent multinodular type, have more significant MVI than do tumors with a smooth margin, such as the single nodular type (these classifications of nodular type are in accordance with the Liver Cancer Study Group of Japan [31]) [2,10,12,33]. The hepatobiliary phase of gadoxetic acid-enhanced MRI has been reported to be useful in the evaluation of the tumor macroscopic type [11]. However, to our knowledge, no previous reports have suggested the usefulness of SI evaluation in the prediction of MVI. For the prediction of MVI in gadoxetic acid-enhanced MRI, gross morphological evaluation may be more suitable than SI evaluation.

Previous reports indicated that a lower ADC can be a useful predictor for MVI during the preoperative evaluation of HCC [22–24]. Suh et al. have evaluated ADCs obtained using *b*-values of 50, 400, and 800 s/mm^2 and determined the best cut-off point for predicting MVI as 1.11×10^{-3} mm^2/s [22]. Additionally, Xu et al. have reported a similar study, limited to small HCCs of less than 2 cm in diameter, and suggested the usefulness of ADCs for predicting MVI even in such small HCCs [23]. They evaluated ADCs obtained using *b*-values of 0 and 500 s/mm^2, and determined the best cut-off point as 1.227×10^{-3} mm^2/s. In the current study, we evaluated the ADCs obtained using *b*-values of 0 and 1000 s/mm^2, and determined the best cut-off point as 1.175×10^{-3} mm^2/s.

Univariate analysis showed that histological grade and ADC were strongly associated with MVI. However, our multiple logistic regression analysis indicated that only ADC was an independent predictor of MVI, similar to the findings of previous reports [22,23].

PD HCC is reported to have a high rate of MVI [32,33]. Therefore, there is a possibility that multicollinearity had occurred in these multiple logistic regression analyses. If ADC reflects an intratumoral factor, it is likely to be histological grade (Fig. 2). However, the reason why ADC stood out as such a strong factor might as well be related to intratumoral factors other than the histological grade.

When evaluating ADCs, it is necessary to consider the influence of microcapillary perfusion [34]. Therefore, we first thought that the reduction of ADC was due not only to the restriction of molecular diffusion, but also to the decrease of capillary perfusion caused by MVI. With increased b-values, the influence of microcapillary perfusion is reduced. However, in our study, we used a higher b-value ($1000 \, \text{s/mm}^2$) than previous reports, so that the influence of microcapillary perfusion is likely to be limited. Therefore, our results suggest that restriction of molecular diffusion caused by MVI itself occurs by an unknown mechanism.

We also analyzed the relationships between the SI and tumor recurrence after hepatic resection. The RFS rate was significantly lower in the low ADC group than in the high ADC group, and there was no significant correlation between the RFS rate and AP-RE or HBP-RE values. From our experience, we believe that these results may be due not only to poor differentiation but also to MVI, both of which were associated with low ADCs. These results indicate that during SI evaluation in gadoxetic acid-enhanced and DWI MRI of small HCCs, ADC evaluation is useful for predicting poor differentiation as well as MVI; moreover, this value was also significantly related to tumor recurrence.

There were some limitations in our study. First, it was retrospective and involved a small number of patients; therefore, there is a possibility that selection bias have occurred. Second, because we enrolled only the cases with hepatic resection, the number of WD HCCs was small. As such, it may be insufficient for assessing statistical significance for the histological grade. Third, ADC measurements can be influenced by patient-related, hardware-related, and sequence-related factors [35]. In our study, we evaluated two models of MRI from different vendors and with different field strengths, namely 1.5 T and 3.0 T MRI. The median ADCs of liver background obtained by using 1.5 T and 3.0 T MRI were 1.32 (range: $1.1–1.72) \times 10^{-3} \, \text{mm}^2/\text{s}$ and 1.26 (range: $0.97–1.47) \times 10^{-3} \, \text{mm}^2/\text{s}$, respectively, which were not significantly different ($P = 0.084$). For this reason, we combined the data sets for analysis.

ADC values are dependent on the set b-value and technical parameters. Therefore, the best cut-off point for predicting MVI may differ between facilities. In fact, our cut-off point was close to that previously reported, but yielded a different result. Thus, to use such cut-off point in the clinical setting, it is necessary to standardize the technical protocol. If it is not realistic, it may be necessary to determine the best cut-off point for each facility. Alternatively, whether it would be possible to use other evaluation method, such as the ADC ratio to the background of the liver or other organs, and whether a standardized evaluation is feasible, needs to be determined in future.

In conclusion, during evaluation of SI in gadoxetic acid-enhanced and diffusion-weighted MRI of small HCCs, the ADC is the best predictor of poor differentiation and MVI, and is also significantly related to tumor recurrence. These findings imply that evaluation of ADC will be useful for deciding a therapeutic strategy for patients with small HCCs.

Conflict of interest
None declared.

References

[1] El-Serag HB. Epidemiology of viral hepatitis and hepatocellular carcinoma. Gastroenterology 2012;142:1264–73.

[2] Sumie S, Kuromatsu R, Okuda K, et al. Microvascular invasion in patients with hepatocellular carcinoma and its predictable clinicopathological factors. Annals of Surgical Oncology 2008;15:1375–82.

[3] Oishi K, Itamoto T, Amano H, et al. Clinicopathologic features of poorly differentiated hepatocellular carcinoma. Journal of Surgical Oncology 2007;95:311–6.

[4] Pawlik TM, Gleisner AL, Anders RA, et al. Preoperative assessment of hepatocellular carcinoma tumor grade using needle biopsy implications for transplant eligibility. Annals of Surgery 2007;245:435–42.

[5] Takamori R, Wong LL, Dang C, et al. Needle-tract implantation from hepatocellular cancer: is needle biopsy of the liver always necessary. Liver Transplantation 2000;6:67–72.

[6] Huppertz A, Balzer T, Blakeborough A, et al. Improved detection of focal liver lesions at MR imaging: multicenter comparison of gadoxetic acid enhanced MR images with intraoperative findings. Radiology 2004;230:266–75.

[7] Kitao A, Matsui O, Yoneda N, et al. The uptake transporter OATP8 expression decreases during multistep hepatocarcinogenesis: correlation with gadoxetic acid enhanced MR imaging. European Radiology 2011;21:2056–66.

[8] Kim HY, Choi JY, Kim CW, et al. Gadolinium ethoxybenzyl diethylenetriamine pentaacetic acid-enhanced magnetic resonance imaging predicts the histological grade of hepatocellular carcinoma only in patients with Child–Pugh class A cirrhosis. Liver Transplantation 2012;18:850–7.

[9] Kogita S, Imai Y, Okada M, et al. Gd-EOB-DTPA enhanced magnetic resonance images of hepatocellular carcinoma: correlation with histological grading and portal blood flow. European Radiology 2010;20:2405–13.

[10] Eguchi S, Takatsuki M, Hidaka M, et al. Predictor for histological microvascular invasion of hepatocellular carcinoma: a lesson from 229 consecutive cases of curative liver resection. World Journal of Surgery 2010;34:1034–8.

[11] Fujinaga Y, Kadoya M, Kozaka K, et al. Prediction of macroscopic findings of hepatocellular carcinoma on hepatobiliary phase of gadolinium-ethoxybenzyl-diethylenetriamine pentaacetic acid-enhanced magnetic resonance imaging: correlation with pathology. Hepatology Research 2013;43:488–94.

[12] Ariizumi S, Kitagawa K, Kotera Y, et al. A non-smooth tumor margin in the hepatobiliary phase of gadoxetic acid disodium (Gd-EOB-DTPA)-enhanced magnetic resonance imaging predicts microscopic portal vein invasion, intrahepatic metastasis, and early recurrence after hepatectomy in patients with hepatocellular carcinoma. Journal of Hepato-Biliary-Pancreatic Surgery 2011;18:575–85.

[13] Taouli B, Koh DM. Diffusion-weighted MR imaging of the liver. Radiology 2010;254:47–66.

[14] Koh DM, Collins DJ. Diffusion-weighted MRI in the body: applications and challenges in oncology. American Journal of Roentgenology 2007;188:1622–35.

[15] Vandecaveye V, De Keyzer F, Verslype C, et al. Diffusion-weighted MRI provides additional value to conventional dynamic contrast enhanced MRI for detection of hepatocellular carcinoma. European Radiology 2009;19:2456–66.

[16] Xu PJ, Yan FH, Wang JH, et al. Contribution of diffusion-weighted magnetic resonance imaging in the characterization of hepatocellular carcinomas and dysplastic nodules in cirrhotic liver. Journal of Computer Assisted Tomography 2010;34:506–12.

[17] Nishie A, Tajima T, Asayama Y, et al. Diagnostic performance of apparent diffusion coefficient for predicting histological grade of hepatocellular carcinoma. European Journal of Radiology 2011;80:e29–33.

[18] Nakanishi M, Chuma M, Hige S, et al. Relationship between diffusion-weighted magnetic resonance imaging and histological tumor grading of hepatocellular carcinoma. Annals of Surgical Oncology 2012;19:1302–9.

[19] Heo SH, Jeong YY, Shin SS, et al. Apparent diffusion coefficient value of diffusion-weighted imaging for hepatocellular carcinoma: correlation with the histologic differentiation and the expression of vascular endothelial growth factor. Korean Journal of Radiology 2010;11:295–303.

[20] Nasu K, Kuroki Y, Tsukamoto T, et al. Diffusion-weighted imaging of surgically resected hepatocellular carcinoma: imaging characteristics and relationship among signal intensity, apparent diffusion coefficient, and histopathologic grade. American Journal of Roentgenology 2009;193:438–44.

[21] Muhi A, Ichikawa T, Motosugi U, et al. High-b-value diffusion-weighted MR imaging of hepatocellular lesions: estimation of grade of malignancy of hepatocellular carcinoma. Journal of Magnetic Resonance Imaging 2009;30:1005–11.

[22] Suh YJ, Kim MJ, Choi JY, et al. Preoperative prediction of the microvascular invasion of hepatocellular carcinoma with diffusion-weighted imaging. Liver Transplantation 2012;18:1171–8.

[23] Xu P, Zeng M, Liu K, et al. Microvascular invasion in small hepatocellular carcinoma: is it predictable with preoperative diffusion-weighted imaging. Journal of Gastroenterology and Hepatology 2014;29:330–6.

[24] Fidelman N, Qayyum A. Pretransplant prediction of microvascular invasion in patients with hepatocellular carcinoma: added value of diffusion-weighted magnetic resonance imaging. Liver Transplantation 2012;18:1131–3.

[25] Nojiri S, Kusakabe A, Fujiwara K, et al. Noninvasive evaluation of hepatic fibrosis in hepatitis C virus-infected patients using ethoxybenzyl-magnetic resonance imaging. Journal of Gastroenterology and Hepatology 2013;28:1032–9.

[26] Theise ND, Curado MP, Franceschi S, et al. Hepatocellular carcinoma. In: Bosman FT, Carneiro F, Hruban RH, Theise ND, editors. WHO classification of tumours of the digestive system. Lyon: International Agency for Research on Cancer; 2010. p. 205–16.

[27] Matsui O. Imaging of multistep human hepatocarcinogenesis by CT during intra-arterial contrast injection. Intervirology 2004;47:271–6.

[28] Narita M, Hatano E, Arizono S, et al. Expression of OATPIB3 determines uptake of Gd-EOB-DTPA in hepatocellular carcinoma. Journal of Gastroenterology 2009;44:793–8.

[29] Kitao A, Zen Y, Matsui O, et al. Hepatocellular carcinoma: signal intensity at gadoxetic acid-enhanced MR imaging-correlation with molecular transporters and histopathologic features. Radiology 2010;256:817–26.

[30] Kobayashi S, Matsui O, Gabata T, et al. Intranodular signal intensity analysis of hypovascular high-risk borderline lesions of HCC that illustrate multi-step hepatocarcinogenesis within the nodule on Gd-EOB-DTPA-enhanced MRI. European Radiology 2012;81:3839–45.

[31] Liver Cancer Study Group of Japan. The general rules for the clinical and pathological study of primary liver cancer. Tokyo: Kanehara; 2010.

[32] Shirabe K, Itoh S, Yoshizumi T, et al. The predictors of microvascular invasion in candidates for liver transplantation with hepatocellular carcinoma-with special reference to the serum levels of des-gamma-carboxy prothrombin. Journal of Surgical Oncology 2007;95:235–40.

[33] Yamashita Y, Tsuijita E, Takeishi K, et al. Predictors for microinvasion of small hepatocellular carcinoma ≤2 cm. Annals of Surgical Oncology 2012;19:2027–34.

[34] Le Bihan D, Breton E, Lallemand D, et al. Separation of diffusion and perfusion in intravoxel incoherent motion MR imaging. Radiology 1988;168:497–505.

[35] Sasaki M, Yamada K, Watanabe Y, et al. Variability in absolute apparent diffusion coefficient values across different platforms may be substantial: a multivendor, multi-institutional comparison study. Radiology 2008;249:624–30.